2011 American Control Conference
on O'Farrell Street, San Francisco, CA, USA
June 29 - July 01, 2011

Hybrid Large Scale System Model for a DC Microgrid

P. Tulpule*, S. Yurkovich, J. Wang, G. Rizzoni
Center for Automotive Research, The Ohio State University

***Abstract*— A microgrid power system with multiple energy sources and loads is considered in this paper. Such microgrids are common due to the needs of distributed generation, renewable energy, and hybrid power sources. The system under study consists of a large number of power converters operating over a wide range of voltages and currents, interconnected via a distribution network. Stability analysis and supervisory control design requires a good model of the system that considers different operations within the microgrid, such as voltage/current levels, bidirectional power flows, and on/off switching of the power converters.**

In this paper, a state variable modeling approach is presented to develop a hybrid large-scale system model of the microgrid. State variable models of individual converters linearized at different operating points are the building blocks of the model. A large-scale interconnected system model is developed for each feasible interconnection of the linearized models of the converters. The switching model, which is a combination of state based and input based switching events between these large-scale system models, is developed using hybrid system theory. The modeling approach is applied to two example systems consisting of DC-DC converters and a DC bus. The hybrid large scale system models are compared with circuit simulations to show the validity of the modeling process.

I. Introduction

A microgrid consists of multiple energy sources (electrochemical battery, fuel cell, supercapacitors, IC engine generators, PV panels, wind energy, power grid tie, etc.) and multiple loads (DC-DC converters, inverters, motor drives, etc.) connected together through a network of interconnections. A microgrid also consists of local controllers for stability of the network and a supervisory controller to optimize energy utilization.

This work is motivated by control and stability challenges of plug-in electric vehicle (PEV) charging stations with renewable energy sources. The microgrid considered in this paper is shown in Figure 1. The example microgrid for PEV charging station is comprised of three energy sources (renewable energy source, stationary battery storage, and power grid) with their respective power conditioning devices and multiple PEV charging points connected together. Such interconnected systems can be designed in several ways; some examples are given in [1]. There are two important ways to connect these devices. One is using a single power distribution node, where all devices are connected to a common node; the second is via a transmission line, where all devices are connected in a string and power is distributed over the transmission line. DC power distribution is considered between power sources and PEV chargers because the system components are mainly DC devices and DC power distribution provides many benefits over AC distribution, such as higher efficiency, fewer stability issues, etc. The objective of the microgrid energy management controller for PEV charging station is to maximize the solar energy utilization by distributing the charging power of the PEVs throughout the day while satisfying the charging demand.

The first step in solving the associated control problem is to develop a suitable mathematical model of the system. The microgrid is a large scale system ([2]) consisting of many power converters connected together; the microgrid also has properties of hybrid systems [3] - hierarchical control structure, and event based switching (connection/disconnection of loads, changes in power supply configurations - constant current, constant voltage, etc.). Therefore, a combination of the two system types is used to design a hybrid large scale system (HLSS) model of the DC microgrid. The microgrid modeling approaches are considered in the literature using various methods [4], [5], [6], [7] for different applications. The common approach is to model the power converter using transfer functions and then design the controller for stability and energy management. This approach is used in [4] to develop a model of a DC bus and associated converters and used to develop a load distribution strategy. A similar transfer function approach was used in [6] for a hybrid generation system for a AC power source. A concept described as DC-bus signaling based on droop control was presented in [5] to manage the power sharing between different DC sources; in that work, simple transfer function models are used for the design of controllers and use on a system prototype. Majumdar *et al.* [7] used a state variable approach for stability analysis of multi-converter AC microgrid using linearized models and droop control for power sharing. That work requires consideration of system operation when the operating point deviates away from the linear region. Extending these existing works, the modeling method proposed in this paper uses linearized state variable models of DC-DC converters and system interconnections at different system operating points and changing interconnections to develop a large-scale system model of the microgrid. This modeling approach also considers switching between the state variable models due to external control or inherent changes in the system operation.

Hybrid large scale systems arise due to interconnections between sub-systems having multiple modes of operation. Air traffic control, smart-grids, autonomous vehicles/robots are some examples of HLSS. The notion of large scale systems or structured systems [2] is very subjective but typically,

*Corresponding Author: Pinak Tulpule, The Ohio State University, Columbus, Ohio. email: tulpule.1@osu.edu

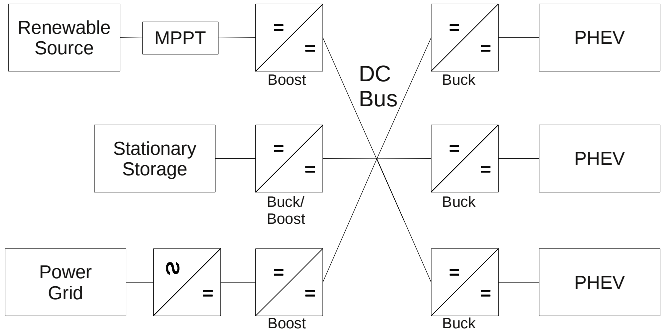

Fig. 1. Schematic of PEV charging station using local renewable energy source.

large scale systems can be decomposed or partitioned into smaller sub-systems and their interconnections. A hybrid system is a dynamical system whose behavior of interest is characterized by interacting continuous and discrete time systems [3]. Hybrid systems can arise naturally (e.g., bouncing ball, cell development process in biology), due to bang-bang control, saturation and hysteresis (e.g., thermostatic control), due to the use of state machine/ computer control of continuous time systems (e.g., automatic gear box) and hierarchical operation of systems (e.g., supervisory control). A detailed investigation of HLSS systems for multi-agent hierarchical control systems involving continuous local controllers and discrete decision making was performed in [8] and some basic properties of HLSS were also developed. Networked large scale systems with hierarchical control design was considered in [9]. That work also considers large scale impulsive systems as a combination of interconnected impulsive sub-systems and stability properties were developed by considering the individual impulsive systems and vector dissipativity theory.

The remainder of this paper is organized as follows. Section II presents a hybrid large scale system model development process for microgrids. Section III presents two case studies, one for a small circuit and another for a microgrid for PEV charging stations. Finally, section IV gives conclusions and future work.

II. Model development

This section presents the model development of the microgrid as a hybrid large scale system of the form,

$$\begin{aligned} \dot{x}(t) &= A_q x(t) + E_q e(t) \\ y(t) &= x(t) \\ q^+ &= f(q^-, x(t), u(t), e(t)) \quad q \in \mathbb{Z} \\ u(t) &= g(y(t), e([t-t_1, t+t_2]), q(t), t) \quad t_1, t_2 \geq 0 \end{aligned} \tag{1}$$

In the above, $x(t)$ is the system state vector, $e(t)$ is the disturbance input vector, u is the control input vector, q is the discrete state of the system, A_q and E_q are families of system matrices indexed by q and q^-, q^+ are discrete states before and after the switching event, respectively. This system has a very special structure in that the control input u is an input to the switching function which determines the discrete state of the system, which in turn determines the system dynamics (A_q and E_q); the control input does not directly affect the continuous time dynamics.

The modeling approach is presented here by considering an example of a PEV charging station as shown in Figure 1; the same approach can be applied to other schematics and converters involving other circuit topologies. The smallest part of the system considered in this work is the DC-DC converter. The dynamics and nonlinearities associated with the PWM switching and the models of smaller components are averaged and/or linearized. The converter can be modeled using different methods [10] depending on the objective of the model, e.g. multi-frequency averaging [11], state space averaging, sampled data modeling, etc. The small signal stability of the converter can be assessed using state-space averaging [12]. The models are further linearized, combined using the interconnection models and a HLSS model is developed.

A. State Space Averaging

The switching converter operates in two intervals, switch "on" and switch "off"; the duration of each is controlled by switching frequency and duty cycle. Therefore, the switching converter can be represented by two state variable systems $(A_{on}, B_{on}, C_{on}, D_{on})$ and $(A_{off}, B_{off}, C_{off}, D_{off})$ corresponding to each interval. If T_{on} is switch "on" interval, T_{off} is switch "off" interval, and $T = T_{on} + T_{off}$ is the switching period, then averaging over one period T results in

$$\dot{x} = Ax + Bu \tag{2}$$

$$y = dy_{on} + (1-d)y_{off} = Cx \tag{3}$$

where, $A = dA_{on} + (1-d)A_{off}$, $B = dB_{on} + (1-d)B_{off}$, $C = dC_{on} + (1-d)C_{off}$ and $d = T_{on}/T$ is the duty cycle. This method is commonly known as "state space averaging" [13]. In [12] the authors argue that the theorems of averaging can be applied to power electronic systems to prove closeness properties of the solutions from state space averaging with those from switching systems. These averaged models can be nonlinear and therefore the nonlinear models are linearized around appropriate operating points. The models of the switching converters can be developed using this approach; for example, consider a boost converter with PI voltage regulator as shown in Figure 2.

Define three states of the converter as capacitor voltage, inductor current, and output of integrator in the voltage regulator. Define states of the linearized state space model as $\mathbf{x} = [\hat{x}_1 \ \hat{x}_2 \ \hat{d}]^T$, and inputs as $\mathbf{u} = [\hat{u}_1 \ \hat{u}_2]^T$ to simplify the notation (note the removal of ˆ from the notation). The system equations are

$$\dot{\mathbf{x}}_{1,v} = A_{1,v}\mathbf{x}_{1,v} + B_{1,v}\mathbf{u}_{1,v} \tag{4}$$

$$\mathbf{y}_{1,v} = \mathbf{x}_{1,v} \tag{5}$$

with

$$A_{1,v} = \begin{bmatrix} 0 & -\frac{1-D}{L} & \frac{X_2}{L} \\ \frac{1-D}{C} & -\frac{1}{RC} & -\frac{X_1}{C} \\ -k_p\frac{1-D}{C} & \frac{k_p}{RC} - k_i & \frac{k_p X_1}{C} \end{bmatrix} B_{1,v} = \begin{bmatrix} \frac{1}{L} & 0 \\ 0 & \frac{1}{C} \\ 0 & -\frac{k_p}{C} \end{bmatrix} \tag{6}$$

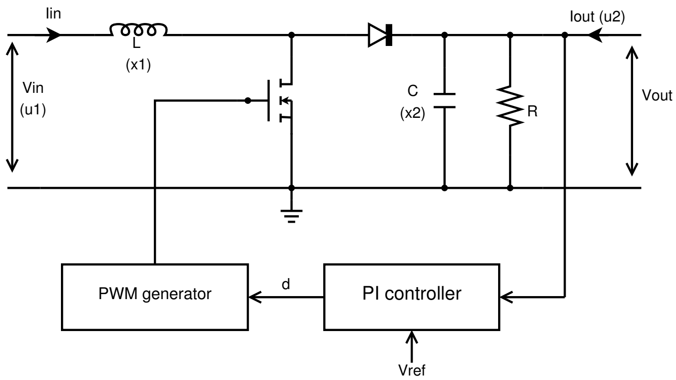

Fig. 2. Circuit diagram of a boost converter along with PI voltage regulator.

where the first subscript represents the converter type (e.g. 1: Boost, 2: Buck) and the second subscript represents the control mode (e.g. v: voltage regulator, c: current regulator). The derivation of these equations is omitted here because this process is very common in power electronics and explained in many references, e.g. [14]. In the same fashion, linearized state variable models for a boost converter with constant current (CC) control, a buck regulator with constant voltage (CV) control, and a buck converter with constant current control can be derived.

B. Large Scale System Representation

Consider a simple power distribution system with one boost converter in CV mode supplying power to one buck converter in CV mode. Now the input current of the buck converter is the load current of a boost converter and the output voltage of a boost converter is the source voltage of the buck converter, therefore,

$$(\hat{u}_2)_{1,v} = -(\hat{x}_3)_{2,v} \tag{7}$$
$$(\hat{u}_1)_{2,v} = (\hat{x}_2)_{1v} \tag{8}$$

Using the vector notation introduced in the last section, $\mathbf{x}_{1,v} = [\hat{x}_1\ \hat{x}_2\ \hat{d}]^T$ and $\mathbf{x}_{2,v} = [\hat{x}_1\ \hat{x}_2\ \hat{x}_3\ \hat{d}]^T$, it is possible to write

$$\frac{d}{dt}\left[\begin{array}{c}\mathbf{x}_{1,v}\\ \hline \mathbf{x}_{2,v}\end{array}\right] = \left[\begin{array}{c|c}A_{1,v} & 0\\ \hline 0 & A_{2,v}\end{array}\right]\left[\begin{array}{c}\mathbf{x}_{1,v}\\ \hline \mathbf{x}_{2,v}\end{array}\right] + \left[\begin{array}{c|c}B_{1,v} & 0\\ \hline 0 & B_{2,v}\end{array}\right]\left[\begin{array}{c}(\hat{u}_1)_{1,v}\\ -(\hat{x}_3)_{2,v}\\ \hline (\hat{x}_2)_{1,v}\\ (\hat{u}_2)_{2,v}\end{array}\right] \tag{9}$$

Combining the states and inputs together and using a superscript to represent the rows and columns of a matrix (e.g., $B^{1:3,2}$ represents rows one to three and the second column of matrix B), we have

$$\frac{d}{dt}\left[\begin{array}{c}\mathbf{x}_{1,v}\\ \hline \mathbf{x}_{2,v}\end{array}\right] = \left[\begin{array}{c|c}A_{1,v} & 0\ \ 0\ \ -B_{1,v}^{1:3,2}\ \ 0\\ \hline 0\ \ B_{2,v}^{1:4,1}\ \ 0 & A_{2,v}\end{array}\right]\left[\begin{array}{c}\mathbf{x}_{1,v}\\ \hline \mathbf{x}_{2,v}\end{array}\right] + \left[\begin{array}{cc}B_{1,v}^{1:3,1} & 0\\ \hline 0 & B_{2,v}^{1:4,2}\end{array}\right]\left[\begin{array}{c}(\hat{u}_1)_{1,v}\\ (\hat{u}_2)_{2,v}\end{array}\right] \tag{10}$$

$$\frac{d}{dt}\begin{bmatrix}\mathbf{x}_{1,v}\\ \mathbf{x}_{2,v}\end{bmatrix} = \begin{bmatrix}A_{1,v} & \tilde{A}_{1,v}\\ \tilde{A}_{2,v} & A_{2,v}\end{bmatrix}\begin{bmatrix}\mathbf{x}_{1,v}\\ \mathbf{x}_{2,v}\end{bmatrix} + \begin{bmatrix}\tilde{B}_{1,v}\\ \tilde{B}_{2,v}\end{bmatrix}\begin{bmatrix}(\hat{u}_1)_{1,v}\\ (\hat{u}_2)_{2,v}\end{bmatrix} \tag{11}$$

where, $\tilde{A}_{1,v} = [0\ 0\ -B_{1,v}^{1:3,2}\ 0]$, $\tilde{A}_{2,v} = [0\ B_{2,v}^{1:4,1}\ 0]$, $\tilde{B}_{1,v} = [B_{1,v}^{1:3,1}\ 0]$, and $\tilde{B}_{2,v} = [0\ B_{2,v}^{1:4,2}\ 0]$. Similarly, for l buck converters and one boost converter, Equations (7) and (8) become

$$(\hat{u}_2)_{1,v} = \sum_{j=1}^{l} (\hat{x}_3)_{2,v}^{j} \tag{12}$$
$$(\hat{u}_1)_{2,v}^{j} = (\hat{x}_2)_{1,v} \quad \forall j = 1,2,3\ldots l \tag{13}$$

where superscript j denotes the j^{th} buck converter. Using the vector notation and following the procedure shown in Equation (9) and (11) the model of the large scale system becomes

$$\frac{d}{dt}\left[\begin{array}{c}\mathbf{x}_{1,v}\\ \hline \mathbf{x}_{2,v}^{1}\\ \vdots\\ \mathbf{x}_{2,v}^{l}\end{array}\right] = \left[\begin{array}{c|ccc}A_{1,v} & \tilde{A}_{1,v} & \ldots & \tilde{A}_{1,v}\\ \hline \tilde{A}_{2,v}^{1} & A_{2,v}^{1} & 0 & 0\\ \vdots & 0 & \ddots & 0\\ \tilde{A}_{2,v}^{l} & 0 & 0 & A_{2,v}^{l}\end{array}\right]\left[\begin{array}{c}\mathbf{x}_{1,v}\\ \hline \mathbf{x}_{2,v}^{1}\\ \vdots\\ \mathbf{x}_{2,v}^{l}\end{array}\right] + \begin{bmatrix}\tilde{B}_{1,v}\\ \tilde{B}_{2,v}^{1}\\ \vdots\\ \tilde{B}_{2,v}^{l}\end{bmatrix}\begin{bmatrix}(u_1)_{1,v}\\ (u_2)_{2,v}^{1}\\ \vdots\\ (u_2)_{2,v}^{l}\end{bmatrix} \tag{14}$$

$$\dot{\bar{\mathbf{x}}} = \bar{A}\,\bar{\mathbf{x}} + \bar{B}\,\bar{e} \tag{15}$$

In this way, different system matrices can be constructed by considering the operating mode of the converter and their interconnections.

C. Hybrid System Representation

To model the effect of mode changes, consider the solar battery charging station with multiple PEVs as shown in Figure 1. In this case the solar power output is predictable but uncontrollable, the output of the other two sources is controllable and the PEV charging current is partially controllable as it depends on the charging profile. Applying the modeling process explained in previous sections for the charging station schematic, equations of the form shown in Equations (14) and (15) are obtained for each combination of power sources and PEV chargers. Consider $\bar{\mathbf{X}}^i$, $\bar{\mathbf{E}}^i$ as i^{th} operating point of the system and $\mathbf{X}$, $\mathbf{E}$ as the system state and input, respectively. Then, the linearized system model at

i^{th} operating point is written as

$$\dot{\bar{\mathbf{x}}}^i = \bar{A}^i\bar{\mathbf{x}}^i + \bar{B}^i\bar{e}^i \qquad 0 \le i \le N \tag{16}$$

$$\bar{\mathbf{x}}^i = \mathbf{X} - \bar{\mathbf{X}}^i \tag{17}$$

$$\bar{\mathbf{e}}^i = \mathbf{E} - \bar{\mathbf{E}}^i \tag{18}$$

The first point in defining this system as a hybrid system is the changing system dimensions. The dimensions of the system matrix $\bar{A}^i$ depend on the number of load converters and the number of active sources. The second point is the dynamics of the individual devices. For safe, stable and robust operation of the parallel DC sources, one of the methods is to keep one source as a voltage regulator (or primary source) and the other sources as constant current sources (or constant power sources). Depending on whether a source is operating as a constant voltage or constant current source, the dynamics of the source converter and also the interconnection matrices will change. Therefore, the system matrix ($\bar{A}^i$) will change numerically as well as dimensionally. The changes in system structure are event based according to actions dictated by the supervisory controller (connection/disconnection of loads), as well as the changes in the solar power output (changes in primary source) and battery charging profile (CC-CV mode changes). This system can be modeled as a hybrid dynamical system consisting of a continuous time model for converters and a discrete state transition equation ($q^- \to q^+$) for changes in the system structure, as given by,

$$\dot{\bar{\mathbf{x}}}^q = \bar{A}^q\bar{\mathbf{x}}^q + \bar{B}^q\bar{e}^q \tag{19}$$

$$q^+ = \Gamma(q^-, \mathbf{X}(k), \mathbf{E}(k)) \tag{20}$$

where, $\mathbf{X}$ is the state vector, $q \in \mathbb{Z}$ is the discrete state of the system, Γ is the transition relation between discrete states of the system, $\bar{A}^q, \bar{B}^q$ are system matrices indexed by q, $k \in \mathbb{R}_{\ge 0}$ is the switching time for discrete configuration, and q^-, q^+ are discrete states before and after the switching event, respectively. This model of hybrid system allows to separate the stability analysis of continuous dynamics and controller design to generate the discrete dynamics. Since, the switching signal is an input of the hybrid system, this model allows the study of stability properties under arbitrary switching by considering the Equation (19). The stability properties provide constraints on the switching signal which is the output of discrete transition relations (Equation (20)). This discrete transition relation is realized as a supervisory controller for energy flow management. The design of the supervisory controller is an open problem and can be addressed through state machine, discrete event system, defining switching surface in state space, etc.

III. Examples

The proposed model is applied to a PEV charging station with renewable energy source as shown in Figure 1. This example system is designed with DC bus voltage of 500V, PEV battery of 320V nominal with level 2 charging (3.3kW charging power), photo-voltaic panels (200V) and stationary storage battery (320V). The photovoltaic panel and stationary storage voltages are examples only and do not represent any particular system. Because the goal of this work is to present a modeling method for a DC microgrid, simple converter topologies, namely, boost and buck converters, are designed with PI regulator for voltage and current control. We note that other circuit topologies can be used to design a microgrid whereas the method presented here can used to develop the HLSS model. Smaller circuits are considered below to present results of the HLSS model developed for the microgrid application. Although, higher number of converters can be modeled as HLSS since the matrices in Equation (14) can be scaled to arbitrary dimensions.

The first example is a simple buck converter with CC to CV mode change, while the second example considers a microgrid with one source (boost converter) and three loads (buck converters). The purpose of these examples is to show the performance of the linearized hybrid large scale system model, and to illustrate that it matches closely with the circuit simulations.

A. Example 1

The modeling approach is applied to a system consisting of a DC-DC converter with constant current (CC) and constant voltage (CV) control modes. An external signal switches the controllers from CC mode to CV mode. The circuit is modeled using two linearized state variable systems $S_1 : \dot{\bar{\mathbf{x}}} = A_1\bar{\mathbf{x}} + B_1\bar{\mathbf{e}}; \bar{\mathbf{y}} = C_1\bar{\mathbf{x}}$ and $S_2 : \dot{\bar{\mathbf{x}}} = A_2\bar{\mathbf{x}} + B_2\bar{\mathbf{e}}; \bar{\mathbf{y}} = C_2\bar{\mathbf{x}}$, one for each control method with $\bar{\mathbf{x}} \in \mathbb{R}^5$. The converter starts in CC mode and at time $t = 1$ the controller switches from CC to CV mode. The state variable models are switched from S_1 to S_2 at $t = 1$ such that $\bar{\mathbf{x}}^2(t = 1) = \bar{\mathbf{x}}^1(t = 1)$, i.e., the initial condition of S_2 is equal to state value of S_1 at the time of switching. The simulation results are shown in Figure 3, where a small difference between the circuit simulations and state variable simulation indicate that the HLSS model of the converter is reasonably accurate.

B. Example 2

This second example looks at a large scale system consisting of one boost converter supplying power to three buck converters as shown in Figure 4. Each converter is modeled with its own state variable representation. Using the method explained in section II, large scale system models are developed for each combination of boost and buck converter and their control modes. Because the buck converters are operating in constant current mode, we use the notation given in the previous section to obtain the system matrix as

$$\bar{A}^1 = \left[\begin{array}{c|ccc} A_{1,v} & \tilde{A}_{1,v} & \tilde{A}_{1,v} & \tilde{A}_{1,v} \\ \hline \tilde{A}^1_{2,c} & A^1_{2,c} & 0 & 0 \\ \tilde{A}^2_{2,c} & 0 & A^2_{2,c} & 0 \\ \tilde{A}^3_{2,c} & 0 & 0 & A^3_{2,c} \end{array}\right] \tag{21}$$

Note that when converter 1 changes from CC mode to CV mode, the system matrix becomes

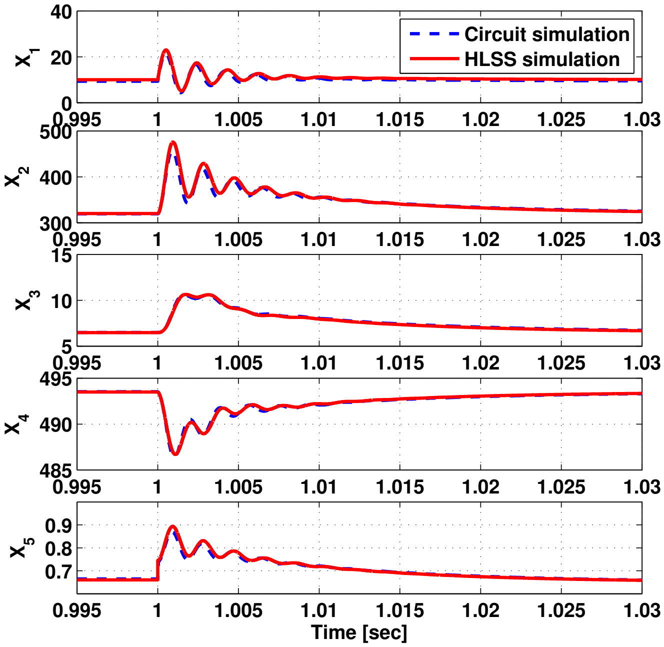

Fig. 3. Comparison between circuit simulation and hybrid large scale system simulation for CC- CV mode change of a buck converter.

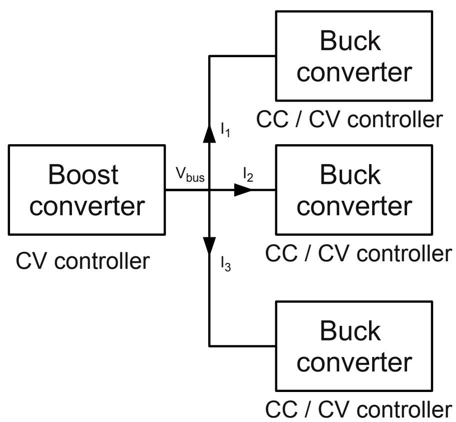

Fig. 4. Schematic of circuit configuration for example 2.

$$\bar{A}^2 = \left[\begin{array}{c|ccc} A_{1,v} & \tilde{A}_{1,v} & \tilde{A}_{1,v} & \tilde{A}_{1,v} \\ \hline \tilde{A}^1_{2,v} & A^1_{2,v} & 0 & 0 \\ \tilde{A}^2_{2,c} & 0 & A^2_{2,c} & 0 \\ \tilde{A}^3_{2,c} & 0 & 0 & A^3_{2,c} \end{array}\right] \tag{22}$$

Note the change in the second row, which corresponds to the first buck converter. Similarly, two other system matrices can be considered for the example system. The switching between different modes of operation causes changes in the system state variable representation. This is achieved by changing the system model from $\bar{A}^1$ to $\bar{A}^2$ at the switching time and assigning proper initial conditions. The simulation results of the transient response when buck converter 1 switches from CC mode to CV mode are shown in Figure 5. The figure gives bus voltage (V_{bus}) and input currents of three buck converters (I_1, I_2, I_3) as shown in Figure 4. The results exhibit a close match between circuit simulations and hybrid large scale system simulations. The output voltage and current of these converters are controlled by the feedback regulators, modeled directly in the state variable representation. Because it is important to study the impact of buck converter mode switching on the overall microgrid and impact on other converters modeled as a large scale system, only the input currents and bus voltages are shown here. Other state variables show very close match between circuit simulations and HLSS simulations. The simulations are carried out for consecutive changes in all three converters from CC to CV mode and the result is shown in Figure 6. At every 0.5 seconds one converter switches from CC mode of operation to CV mode of operation. The impact of the switches on other converters is shown in Figure 6. The dynamic response obtained from HLSS model simulations is almost identical to the circuit simulations, except for small differences in bus voltage due to ripple voltage.

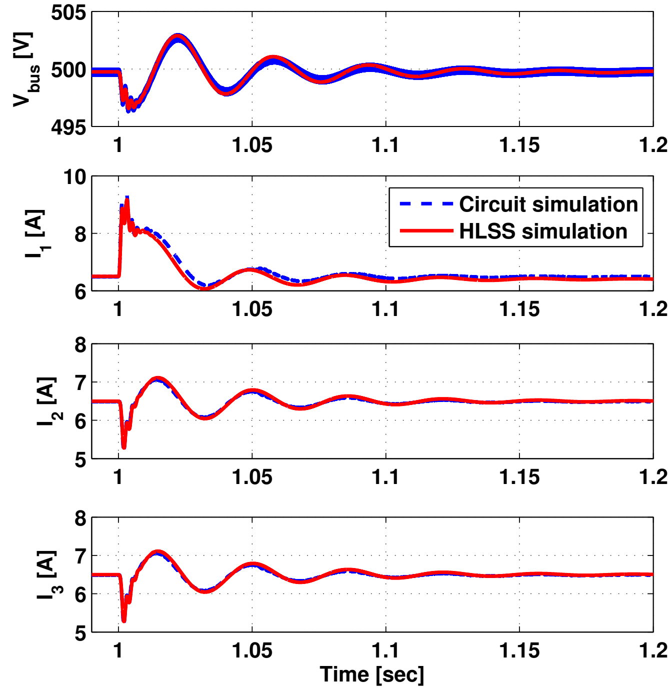

Fig. 5. Comparison between circuit simulation and hybrid large scale system simulation for a microgrid shown in Figure 4.

IV. Conclusion

This paper presents a hybrid large scale system model of a DC microgrid consisting of multiple switching converters. State space averaged models of switching converters are considered with voltage and current regulators. Switching between different modes of operation, and connection/disconnection of converters is modeled through hybrid system methods. The models consider changes in system state-space and also changes in the system dimensions. The modeling method is verified by comparing the transient responses of the state variable model simulations with circuit

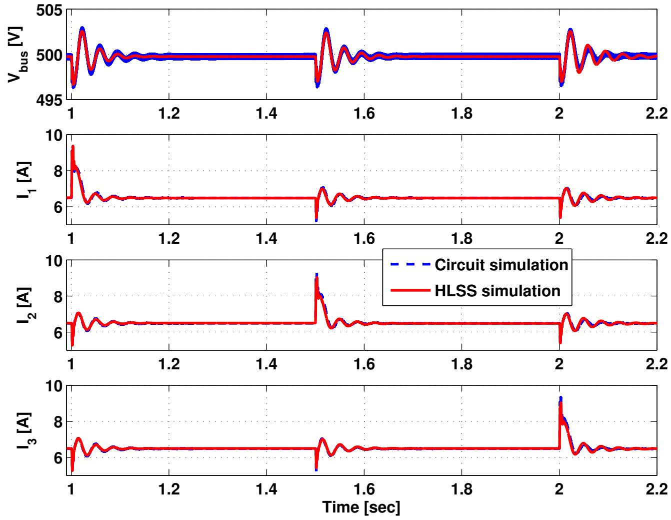

Fig. 6. Comparison between circuit simulation and hybrid large scale system simulation for a microgrid shown in Figure 4.

simulations for mode switching. The hybrid large scale system models developed in this paper can be applied to other system configurations and different converter types including AC and DC systems. The model developed in this paper can be further used to study system stability, design local controllers and design of switching supervisory controllers for microgrids.

References

[1] W. Kramer, S. Chakraborty, B. Kroposki, and H. Thomas, "Advanced power electronic interfaces for distributed energy systems, Part 1: Systems and topologies," National Renewable Energy Laboratory, Tech. Rep. NREL/TP-581-42672, March 2008.

[2] D. Šiljak, *Large scale dynamic systems stability and structure*. Dover Publications, Inc., 2007.

[3] J. Lunze and F. Lamnabhi-Lagarrigue, Eds., *Handbook of hybrid systems control - Theory, tools and applications*. Cambridge University Press, 2009.

[4] P. Karlsson and J. Svensson, "DC bus voltage control for a distributed power system," *IEEE Transactions on Power Electronics*, vol. 18, no. 6, pp. 1405–1412, November 2003.

[5] J. Schonberger, R. Duke, and S. Round, "DC-bus signaling: A distributed control strategy for a hybrid renewable nanogrid," *IEEE Transactions on Industrial Electronics*, vol. 53, no. 5, pp. 1453–1460, October 2006.

[6] S. K. Kim, J. H. Jeon, C. H. Cho, J. B. Ahn, and S. H. Kwon, "Dynamic modeling and control of a grid-connected hybrid generation system with versatile power transfer," *IEEE Transactions on Industrial Electronics*, vol. 55, no. 4, pp. 1677–1688, April 2008.

[7] R. Majumdar, A. Ghosh, G. Ledwich, and F. Zare, "Stability analysis and control of multiple converter based autonomous microgrid," in *IEEE international conference on control and automation, New Zealand*, December 2009.

[8] J. Lygeros, "Hierarchical, hybrid control of large scale systems," Ph.D. dissertation, University of California at Berkeley, 1996.

[9] Q. Hui, "Nonlinear dynamical systems and control for large-scale, hybrid, and network systems," Ph.D. dissertation, Georgia Institute of Technology, 2008.

[10] D. Maksimović, A. M. Stanković, V. J. Thottuvelil, and G. C. Verghese, "Modeling and simulation of power electronic converters," *Proceedings of the IEEE*, vol. 89, no. 6, pp. 898–912, June 2001.

[11] V. Caliskan, G. C. Verghese, and M. Stanković, "Multifrequency averaging of DC/DC converters," *IEEE Transactions on Power Electronics*, vol. 14, no. 1, pp. 124–133, January 1999.

[12] P. T. Krein, J. Bentsman, R. M. Bass, and B. L. Lesieutre, "On the use of averaging for the analysis of power electronic systems," *IEEE Transactions on Power Electronics*, vol. 5, no. 2, pp. 182–190, April 1990.

[13] R. D. Middlebrook and S. Ćuk, "A general unified approach to modelling switching-converter power stages," *International Journal of Electronics*, vol. 42, no. 6, pp. 521–550, June 1977.

[14] D. Mitchell, *DC-DC Switching Regulator Analysis*. McGraw Hill, 1988.